

## **Electronic Supplementary Information (ESI) for:**

### **Detection of Bivalent Mn Ions by A pH-adjustable Recognition Method via Quantum Dots Fluorescence Sensing**

Shuhong Xu, Chunlei Wang, Haisheng Zhang, Qingfeng Sun, Zhuyuan Wang, Yiping

Cui\*

[\*] Prof. Y. P. Cui, Dr. S. H. Xu, C. L. Wang, Q. F. Sun, H. S. Zhang, Z. Y. Wang,  
Advanced Photonics Center, School of Electronic Science and Engineering, Southeast  
University, Nanjing 210096 (P. R. China)

E-mail: [cyp@seu.edu.cn](mailto:cyp@seu.edu.cn)

**Figure S1.** UV-vis and PL spectra of TG-capped CdTe QDs.

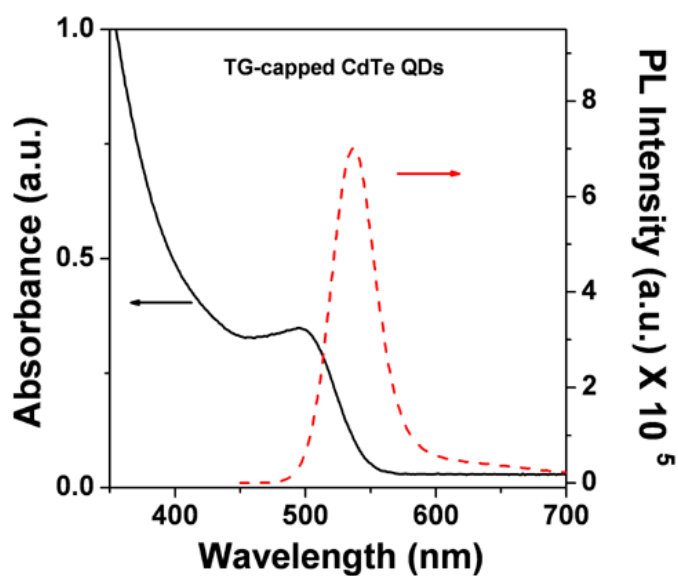
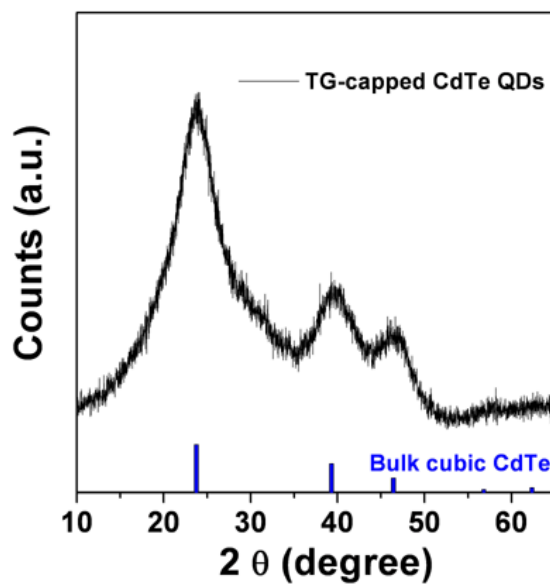
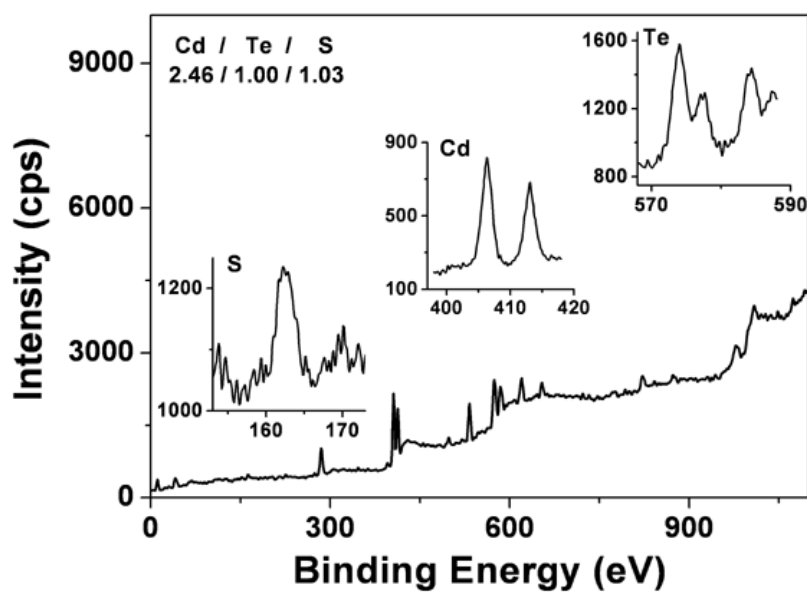


**Figure S2.** XRD pattern of as-prepared TG-capped CdTe QDs.



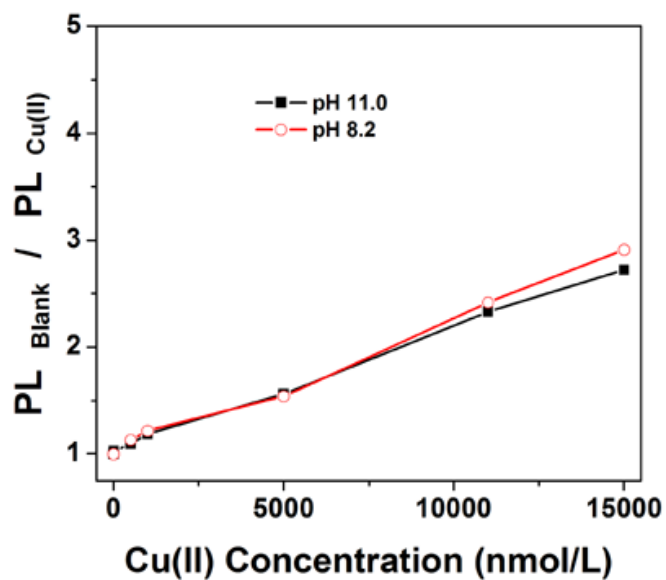
The measured diffractive peaks at 23.8, 39.5, and 46.4 degrees correspond to the zinc blende structure of cubic CdTe bulky crystals.

**Figure S3.** XPS results of as-prepared TG-capped CdTe QDs.



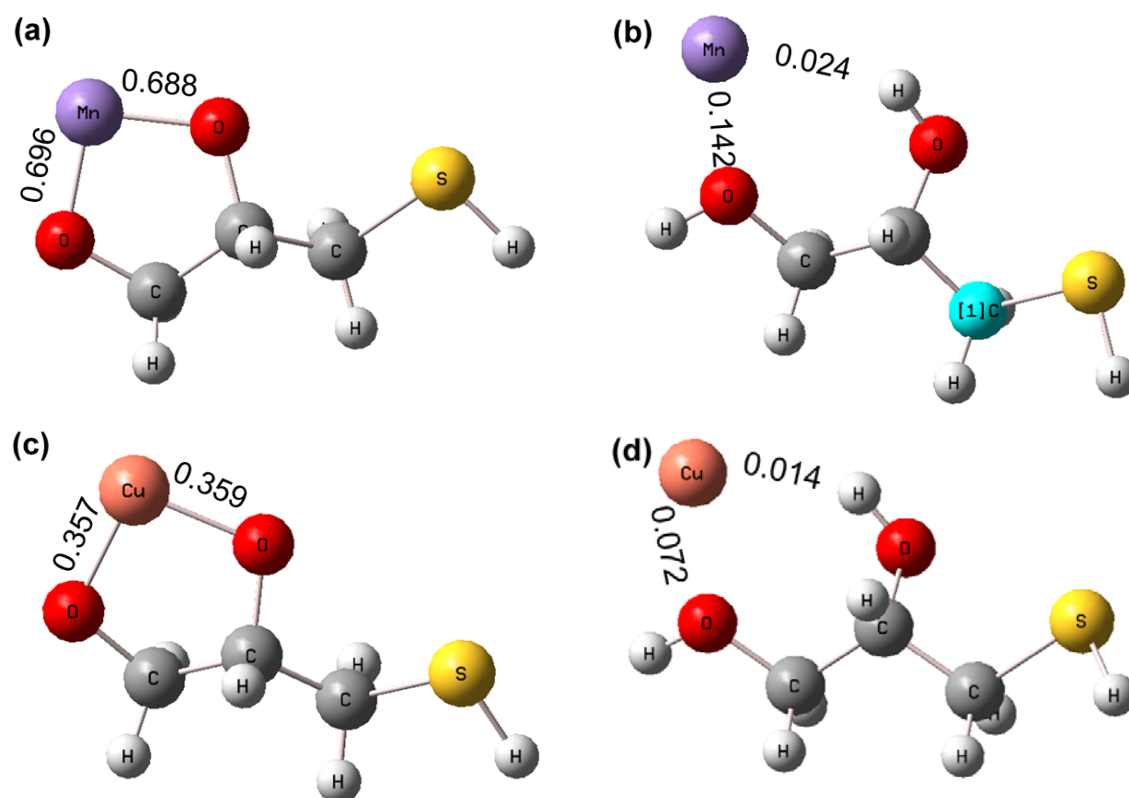
Since QDs were purified via 2-propanol-based precipitation technique before XPS characterization, the measured atom ratio only reflected the composition of QDs. S atoms came from the TG ligand of NCs. According to the atomic ratio of Cd/Te/S (2.46/1.00/1.03), Cd atoms were more than Te atoms. This suggested that the surface of QDs was rich in Cd-TG complexes.

**Figure S4.** PL ratio between blank sample and QDs fluorescence sensing after addition of Cu(II) versus the concentration of Cu(II) at pH 8.2 buffer solution and pH 11.0 buffer solution.



As can be seen, we do not see obvious different preserved PL ratios at pH 8.2 and pH 11.0 after addition of Cu(II) in a broad concentration scope (10-15000 nmol/L). This further indicates the detection process of Cu(II) is not pH-dependent.

**Figure S5.** Theoretical calculation of the adsorption capacity of Mn(II) with negatively charged TG (a) or uncharged TG (b), and the adsorption capacity of Cu(II) with negatively charged TG (c) or uncharged TG (d).



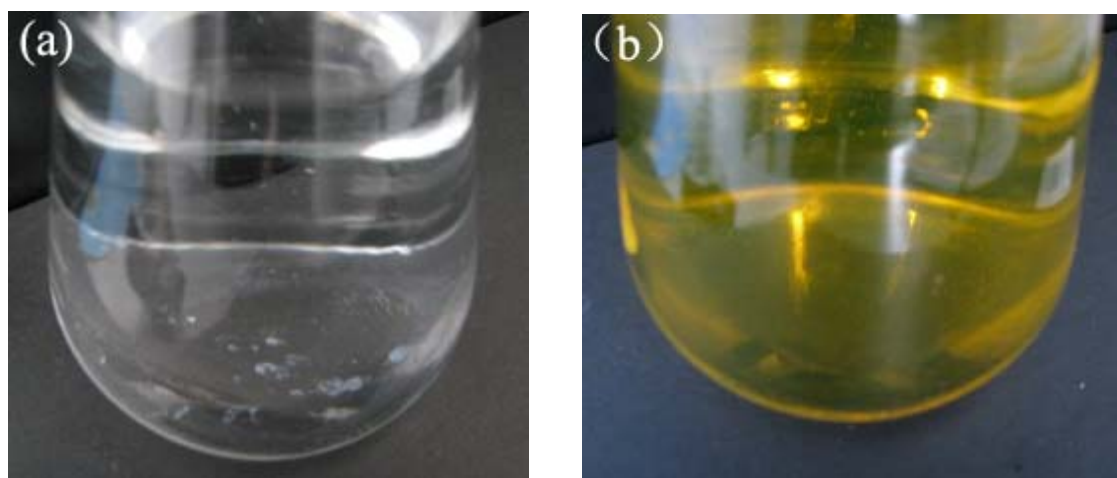
For simulating the adsorption capacity, the structures of Mn(II) or Cu(II) with TG were optimized by a DFT/Lanl2dz method in the Gaussian 03 software according to previous work (J. Phys. Chem. C 2009, 113, 827.). Natural Bond Orbital (NBO) is a function in Gaussian 03 software, which can be used for marking the bond strength between atoms in various optimized molecular structure. The larger bond strength represents the stronger coordination capacity. The calculated results suggest the bond strength of Mn(II) with negatively charged TG in (a) is about 8.3 times as large as the adsorption capacity of Mn(II) with uncharged TG in (b).

**Figure S6.** Photograph of ultrafiltration tubes.



2 mL solution was added into the small filtration tube (left tube with molar weight of 10000 for the mesh), and then was insert into the centrifugation tube (middle tube). After screwing the lid, the tube (right tube) was centrifuged for 30 min at a speed of 4000 r/min. Most of solution can pass through the mesh of the small filtration tube and collected by the centrifugation tube, which was used for ICP measurement. QDs can not pass through the mesh of filtration tube, and thus be leaf in the insert small filtration tube.

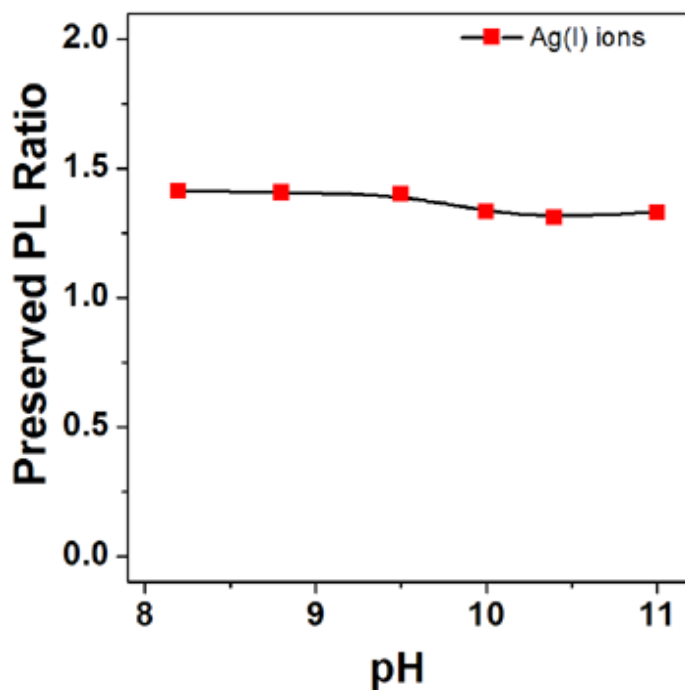
**Figure S7.** Photograph of addition of  $10 \mu\text{mol}\cdot\text{L}^{-1}$  Mn(II) ions into pH 11.0 buffer solution (a) and pH 11.0 buffer solution containing QDs (b).



As can be seen, white  $\text{Mn}(\text{OH})_2$  precipitates will form after addition of  $10 \mu\text{mol}\cdot\text{L}^{-1}$  Mn(II) ions into pH 11.0 buffer solution. However, if QDs exist in pH 11.0 buffer solution, there are no precipitates in solution. It suggests that the presence of QDs restrains the formation of  $\text{Mn}(\text{OH})_2$  precipitates.

Actually, according to the explicit structure of TG-capped QDs in Scheme 1, there is a large amount of negatively charged  $\text{TG}(\text{RO}^-)$  on the surface of QDs, leading to local high concentration of negative charge on QDs. Consequently, the electrostatic attraction between QDs and positively charged Mn(II) ions is much stronger than that between free  $\text{OH}^-$  and Mn(II). Once Mn(II) ions diffuse to the adsorbed layer of QDs, Mn(II) will coordinate with negatively charged  $\text{TG}(\text{RO}^-)$  on QDs due to their strong coordination capacity (Figure S4) and the local high concentration of TG ligands on QDs. This should be the reason why no  $\text{Mn}(\text{OH})_2$  precipitates appear in picture (b).

**Figure S8.** The preserved PL ratio of QDs fluorescence sensing at different pH of buffer solution after addition of  $10 \mu\text{mol}\cdot\text{L}^{-1}$  Ag(I) ions.



As can be seen, the preserved PL ratio shows no obvious change during Ag(I) detection at different pH values. This behavior is the same to the observations during Cu(II) detection. Therefore, it is also possible to discriminate Mn(II) from Ag(I) via similar pH-adjustable recognition method. Moreover, the detection result of Ag(I) is also a proof for the proposed detection mechanism. Due to the much lower solubility of  $\text{Ag}_2\text{Te}$  than CdTe, the substitution reaction is allowed. Since this reaction is not pH-dependent, the detection of Ag(I) is also not pH-dependent.



**Table S1.** XPS results for the precipitates after addition of NaHTe into the mixture of  $\text{Cd}^{2+}$  and  $\text{Mn}^{2+}$  or the mixture of  $\text{Cd}^{2+}$  and  $\text{Cu}^{2+}$  under  $\text{N}_2$  atmosphere. The feed ratio of  $\text{Cd} / \text{Mn}(\text{or Cu}) / \text{Te}$  was 1.0 / 1.0 / 0.50 and the concentration of  $\text{Cd}^{2+}$  was 0.05 mol/L.

<b>Sample</b>	<b>Atomic Ratio</b>
<b><math>\text{Cu}^{2+} + \text{Cd}^{2+}</math></b>	<b>Cu/Cd 17/1</b>
<b><math>\text{Mn}^{2+} + \text{Cd}^{2+}</math></b>	<b>Mn/Cd 0.46/1</b>

Since there are no solubility product constant for CdTe, CuTe and MnTe, we can only use an experiment to compare the relationship between their solubility product constant. As can be seen from the table, in the same concentration of  $\text{Cu}^{2+}$  and  $\text{Cd}^{2+}$ ,  $\text{Te}^{2-}$  preferentially reacted with  $\text{Cu}^{2+}$ , which suggested a much smaller solubility product constant of CuTe than CdTe. As a result, the addition of  $\text{Cu}^{2+}$  into CdTe QDs will lead to the substitution of Cd in CdTe QDs (process 3 in Scheme 1).

In comparison, in the same concentration of  $\text{Mn}^{2+}$  and  $\text{Cd}^{2+}$ ,  $\text{Te}^{2-}$  preferentially reacted with  $\text{Cd}^{2+}$ , which suggested a much smaller solubility product constant of CdTe than MnTe. As a result, the addition of  $\text{Mn}^{2+}$  into CdTe QDs will not lead to the substitution reaction. The detection of  $\text{Mn}^{2+}$  only occurs by processes 1 and 2 in Scheme 1.